Predeposition plasma nitridation process applied to Ge substrates to passivate interfaces between crystalline-Ge substrates and Hf-based high-*K* dielectrics

G. Lucovsky,[a] J. P. Long, K.-B. Chung, H. Seo, B. Watts, R. Vasic, and M. D. Ulrich
Department of Physics, North Carolina State University, Raleigh, North Carolina 27695-8202

(Received 13 October 2008; accepted 29 December 2008; published 9 February 2009)

Interfaces between crystalline-Si and high-*K* Hf-based oxide gate dielectrics have a lower-*K* interfacial transition region (ITR), generally 0.6–0.8 nm SiON, which prevents reactions between Si and Hf precursors used in film deposition. These ITRs contribute ~0.35 nm to the equivalent oxide thickness limiting aggressive scaling. This article addresses Hf-based high-*K* gate dielectrics for devices on crystalline Ge substrates. The band gaps of GeO_2 and Ge_3N_4 are reduced with respect to their Si counterparts, and as such may contribute to increased levels of interfacial defect states. A novel processing sequence is presented for (i) depositing HfO_2 and Hf Si oxynitrides (HFSiON) onto N-passivated Ge(111) and Ge(100), and subsequently (ii) removing Ge–N interfacial bonding during 800 °C thermal annealing in Ar. Near edge x-ray absorption spectroscopy and medium energy ion scattering measurements have confirmed that the interfacial nitrogen is indeed removed. However, there are reactions between the Ge substrate and deposited high-*K* dielectrics, as deposited and after annealing to 600–800 °C, Ge–O bonding into the high-*K* gate stacks which result in increased levels of conduction band edge defect states that incorporate these Ge atoms.
 [DOI: 10.1116/1.3072917]

I. INTRODUCTION

There has been considerable interest in Ge for applications in scaled complementary metal-oxide semiconductor (CMOS) devices,[1–4] particularly for *p*-metal oxide semiconductor field effect transistors (*p*-MOSFETs) for which the hole channel mobility is significantly larger than that of Si. These studies have generally employed Ge native dielectrics GeO_2, GeON, and Ge_3N_4, as interfacial transition regions (ITRs) between the Ge substrate and high-*K* dielectric. *p*-MOSFETs fabricated on Ge with native Ge-ITRs and high-*K* dielectrics such as HfO_2 and ZrO_2 have displayed performance acceptable for integration into scaled CMOS,[3,4] with interfacial defect/trap densities $< \sim 5 \times 10^{11}$ cm^{-2}.

In marked contrast, our previously reported study of *n*-MOS capacitors (*n*-MOSCAPS) with a *n*-Ge/GeO_2/SiO_2 gate stack heterostructure displayed a high density of interfacial negative trapped charge $> 5 \times 10^{12}$ cm^{-2}.[5] More recently, *n*-MOSFETs with Ge_3N_4 or GeON ITRs and HfO_2 and ZrO_2 high-*K* gate stacks have also displayed defect densities, $> 5 \times 10^{12}$ cm^{-2} at the negatively biased Ge substrate/gate dielectric interfaces, and these are too high for CMOS device applications.[3,4] None of these studies has identified the defect bonding arrangements associated with these high levels of interfacial trapping, for example an interfacial Ge dangling bond. Previously reported studies from our group have suggested that the increased levels of trapping at Ge substrates which are negatively biased results from an interfacial gate stack alignment in which the conduction band offset energy between the Ge substrate and a native Ge dielectric ITR is less than that of the conduction band offset energy (CBOE) between a Hf- or Zr-based high-*K* dielectric and the Ge substrate.[6] This arrangement can lead to the formation of a potential well that localizes and confines electrons at the interface, and thereby accounts for high interfacial densities of negative trapped charge.

A novel remote plasma processing sequence that has the potential for eliminating native Ge dielectrics ITRs that *bridge* Ge/high-*K* dielectric interfaces is presented. This article combines spectroscopic and medium energy ion scattering (MEIS) studies to track the evolution of bonding at this interface, and demonstrates that it cannot suppress interfacial reactions during film deposition, and subsequent postdeposition annealing. The details of the absence of any significant interfacial Ge oxide, nitride, or oxynitride has been verified spectroscopically, and preliminary measurements have indicated that this atomic level control of interfacial bonding has resulted in improved electrical performance.[7]

II. EXPERIMENTAL PROCEDURES

HfO_2 films were deposited by 300 °C remote plasma-enhanced chemical-vapor deposition onto remote plasma-nitrided Ge substrates,[6,7] and compared to the same dielectrics deposited onto Si substrates with ~0.6–0.8 nm thick SiON interfacial layers.[8,9] Prior to plasma processing native oxides were removed by wet chemistry techniques that have been optimized for Ge substrates using visible/vacuum ultraviolet spectroscopic ellipsometry, and are qualitatively different than conventional wet chemical processing for Si substrates; i.e., they are generally less acidic in nature.[10,11] Ge-dielectric films were studied spectroscopically as deposited at 300 °C, and annealed to temperatures between 600 and 800 °C. Near edge x-ray absorption spectroscopy (XAS)

[a]Electronic mail: gerry_lucovsky@ncsu.edu

measurements were performed at the Stanford Synchrotron Research Laboratory in the spectral regimes of the O K_1 and N K_1 edges, 520–550 eV, and 390–430 eV, respectively. These XAS measurements have revealed molecular orbital final states for transitions from O 1*s* or N 1*s* core states to O 2*p** or N 2*p** final states, respectively, that have contributions, or projections from near-neighbor Hf 5*d*, 6*s* and 6*p* states.[12] Conduction band edge defect states are also detected in these XAS spectra.[7–13] When detected in MOSCAPs or MOSFETs prior to accelerated current, or voltage stressing, these defects have been referred to as *pre-existing* defects to contrast them with defect produced by stressing. In the remainder of the article these defects will simply be designated as conduction and valence band edge defects. Complementary spectroscopic measurements have been made at the National Synchrotron Light Source at Brookhaven National Laboratory in the UV or soft-x-ray regime between 40 and 130 eV using photoemission spectroscopy, designated as SXPS, XPS, and sometimes UPS.[14]

III. INTERFACIAL BONDING RESULTS

A. Bonding and chemical stability of buried Ge dielectric interfaces

Figure 1(a) displays the results of XPS measurements for HfO_2 on Ge(111) substrates, comparing spectra of films as deposited at 300 °C and after an 800 °C 1 min rapid thermal annealing in Ar. In Fig. 1(a), both spectra include similar valence band and Hf 4*f* features; however, there are differences in band edge defects, and deeper core states associated with Hf and Ge. The shoulder on the low energy side of valence band is larger after the anneal indicating an increase in the defect density.[8,9,14,15] This is addressed in more detail in Sec. IV, where similar increases with annealing temperature also occur for conduction edge defect states as well. These band edge defects are associated with empty and occupied states of the same defect; that have been assigned in Refs. 8 and 9 to O-atom divacancies clustered on internal grain boundaries between nanograins of HfO_2. The core states features in the as-deposited films are for spin-orbit split Hf $5p_{1/2}$ and Hf $5p_{3/2}$ states, while the dominant feature in the 800 °C annealed film for a Ge 3*d* states.[16] Other aspects of these spectra, e.g., the contribution of Hf $5p_{3/2}$ states in the same spectral range as the Ge 3*d* feature, as well as a high energy weak shoulder on the Ge 3*d* state which is attributed to a higher oxidation state of Ge that than the spectral peak at lower eV,[16] will be addressed in detail in a subsequent publication.[15] Qualitatively similar spectra have been obtained on Ge(100) substrates with substrate oxidation effectively suppressed in the as-deposited films, but with reactions between the HfO_2 and Ge substrate resulting in Ge incorporation in the film for annealing temperatures of $\geqslant$700 °C.

Figure 1(b) displays XPS results for HfSiON on Ge(100) as-deposited, and Ge(111) after a 700 °C annealing. There is no evidence for subcutaneous oxidation of Ge during film deposition at 300 °C; however after the 700 °C, there is a Ge 3*d* feature similar to that observed in HfO_2 after the

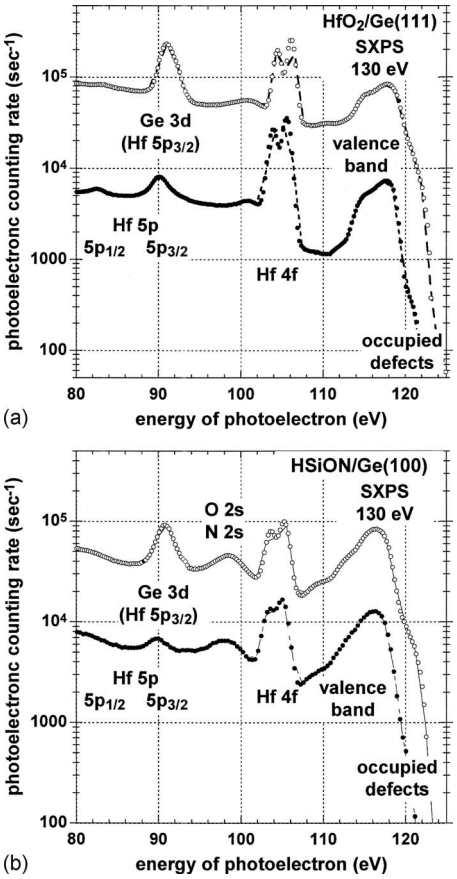

FIG. 1. C. SXPS spectra: (a) for HfO_2 deposited onto Ge(111) as deposited at 300 °C and after an 800 °C 1 min rapid thermal annealing in Ar, and (b) for a high Si_3N_4 content Hf Si oxynitride alloy, $(HfO_2)_{0.3}(SiO_2)_{0.3}(Si_3N_4)_{0.4}$, as deposited on Ge(100) as deposited at 300 °C and after an 800 °C 1 min rapid thermal annealing in Ar. The solid circles in the power traces are as deposited, and the open circles in the upper traces are after the 800 °C annealings.

800 °C annealing. In addition, both spectra show a broad feature that includes contributions for O 2*s* states on the higher side, and N 2*s* states on the low energy side, consistent with the alloy composition this high Si_3N_4 content Hf Si oxynitride alloy (HfSiON): $(HfO_2)_{0.3}(SiO_2)_{0.3}(Si_3N_4)_{0.4}$.[15,16]

B. MEIS: Elimination of interfacial Ge–N bonding during postdeposition annealing

This issues of (i) Ge–N removal, and (ii) the formation of Ge–O bonding in the HfO_2 gate stacks on Ge have in large part been resolved by the recently obtained MEIS results that are presented in Fig. 2.[17] The experimental details relating to the MEIS measurements have been addressed in Ref. 18. These results have revealed significant differences in the incorporation of Ge into the gate stack profiles for HfO_2 and HfSiON after high temperature 800 °C annealings, as well.

Consider first the as-deposited stacks. The N incorporation at the Ge-dielectric interfaces is a direct result of the remote plasma nitridation process that has been used prior to film deposition. Whereas XPS and XAS spectra did not detect Ge–O or Hf–O bonding in the interfacial transition layer of as-deposited films, the respective MEIS spectra clearly

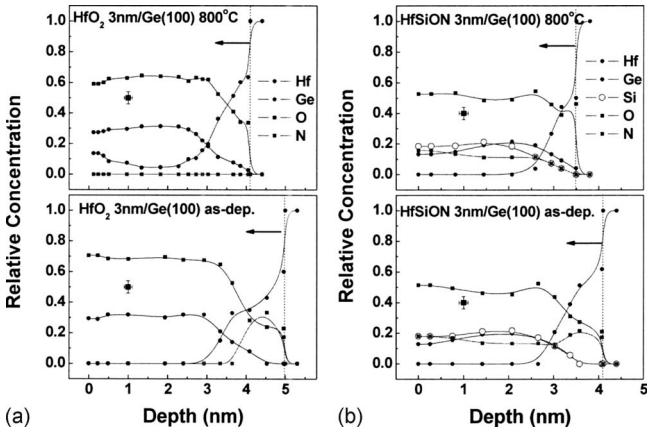

FIG. 2. Compositional depth profile obtained by simulating MEIS energy spectra for as-deposited and annealed (a) HfO_2 films and (b) HfSiON films on Ge(100) substrates. Dotted line and arrow indicate the Ge substrates and the direction of the films. The point with the error bars represents the fitting errors in the depth direction and relative concentration.

indicate that the remote plasma-nitridation process did not completely protect the Ge substrate from subcutaneous oxidation during the respective dielectric deposition processes. This is a significant issue with respect to the processing sequence used in these studies. We are currently developing an alternative approach that attempts to use a superficial nitrided Si layer to suppress subcutaneous oxidation of the Ge during film deposition.

Consider next the annealed films. First, the N atoms introduced during the remote plasma-assisted predeposition nitridation process are no longer evident as a distinct feature at the Ge-dielectric stack interface. However, there is bonded O at the Ge-dielectric interface; the question that must be resolved relates to the bonding of these O atoms: are these O atoms to both Hf and Ge, or just to Hf or Ge. The next significant aspect of the MEIS results is the difference in penetration of Ge into the overlying Hf dielectrics. The defect level differences between HfO_2, HfSiON and HfO_2/HfSiON dielectrics clearly reflects this quantitative difference in Ge transport into, and new defect bonding arrangements as well.

There is a significant transport of Ge into and through the HfO_2 film, where as the transport of Ge is effectively blocked by the noncrystalline HfSiON film. This appears to be the root cause of the difference in bulk defects as discussed in Sec. IV of this article. This difference is one of the more significant issues in the processing of gate stacks on Ge substrates.

One obvious solution to this problem, as well as preventing subcutaneous oxidation of Ge during deposition of oxide dielectrics is to use thin Si layers between the Ge substrate and these oxide dielectrics. This was first demonstrated in Refs. 19 and 20 by Hattangady *et al.* at the Research Triangle Institute (RTI). This approach has been addressed by several other research groups, most notably, the group of Professor

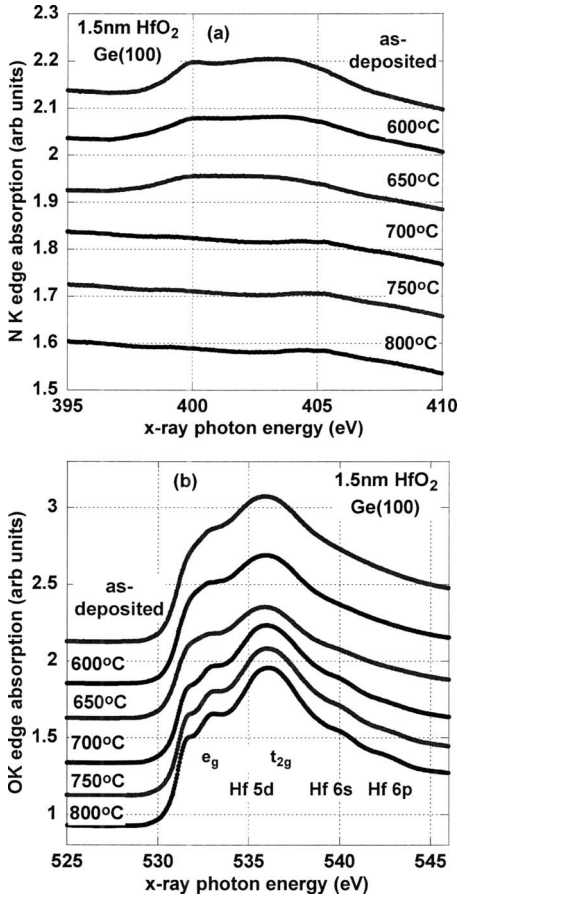

FIG. 3. (a) N K_1 spectra and (b) O K_1 spectra for a 1.5 nm HfO_2 film on a Ge(100) substrate, as deposited at 300 °C, and annealed to 600, 650, 700, 750, and 800 °C.

Krishna Saraswat at Standford University, whose contributions to Ge device processing have been presented in a recent review.[21]

C. XAS N K and O K versus processing temperature

Figure 3(a) are the N K_1 edge XAS spectra for a 1.5 nm thick HfO_2 film deposited onto a plasma-nitrided Ge(100) surface at 300 °C, and Fig. 3(b) are the O K_1 edge spectra for the same film. The spectra in Figs. 3(a) and 3(b) are presented as a function of the processing temperature; as deposited at 300 °C, and annealed at temperatures of 600, 650, 700, 750, and 800 °C. As indicated in the Handbook of Chemistry and Physics,[22] Ge–N bonds decompose in Ge_3N_4 at 450 °C, and sublime from a *Ge subnitride*, approximately Ge_3N_2 at 650 °C. The interfacial nitridation is superficial and extends over about three molecular layers suggesting that elimination of Ge–N in the N K edge spectrum should decrease significantly after an annealing at 650 °C.[6,7,17] This is indeed the case for the 1.5 nm thick HfO_2 film on Ge(100) in Fig. 3(a) where Ge–N bonding is evident in the as-deposited film, and the film after being annealed at 600 and 650 °C. In particular, there are decreases in the Ge–N absorption by about factors of ~25%–30% and >50%, respectively for the 600 and 650 °C annealings. In contrast,

anneals at temperature ⩾700 °C yield spectra that are essentially the same as the background spectrum for a nitrogen free surface, e.g.; the N K_1 edge as obtained for a 1.5 nm thick SiO_2 film on Si, where no N is present in this heterostructure. Qualitatively similar N K_1 spectra have also obtained for 3.0 nm thick HfO_2 on Ge(100), as well as 1.5 and 3 nm thick HfO_2 on Ge(111). These results are consistent with MEIS results that compared as-deposited HfO_2 gate stacks, and HfO_2 gate stacks that have been annealed at 800 °C.[17]

There are qualitative changes in the O K spectra in Fig. 3(b) between the as-deposited, 600 and 650 °C annealed HfO_2 films of Ge substrates, and those annealed at temperatures ⩾700 °C. For the films annealed at temperatures ⩾700 °C, there are spectroscopic features that have been assigned to transitions from the O 1s state, to O 2p π^* states that are mixed in symmetry adapted linear combinations of the atomic states of Hf, 5d, 6s, and 6p.[12] The Hf features assigned to Hf atom final states are indicated in Fig. 3(b). The focus will be on the two features clearly discernable in the band edge 5d e_g Jahn-Teller split doublet state.[8,9] This doublet structure is clearly observed in films annealed at temperatures ⩾700 °C, and correlates with changes in the band edge defects to be addressed in Sec. IV.

IV. SPECTROSCOPIC DETECTION OF CONDUCTION BAND EDGE DEFECTS

This section focuses on conduction band edge defects as determined from spectroscopic studies, mostly from XAS, with a confirmation of assignments based on spectroscopic ellipsometry (SE). There are two ways to obtain detect features from the XAS spectra:[8] (i) by differentiation, and (ii) by Gaussian fitting, and these have been tested and give essentially the same results. The energies of these defect states with the band gap of HfO_2 will be referenced to the e_g band edge states. This focus is mainly on HfO_2, but important comparisons with also be made with HfSiON and HfO_2/HfSiON stacked dielectrics.

Figure 4 is a second derivative O K_1 edge spectrum for a 1.5 nm thick HfO_2 film on Ge(100) annealed to 800 °C. Two band edge defect features are indicated in red in a 10× spectrum, the Hf 5d e_g doublet features, and the Hf 5d t_{2g} triplet features blue. The relative defect state energies, and their energies with respect to the the lowest e_g feature will be used in comparisons with Gaussian fitting of the same O K_1 spectra. The defect state splitting is 1.7 ± 0.15 eV, and the energy difference between the higher x-ray energy defect and the lower x-ray energy e_g state is 1.8 ± 0.15 eV.

Figures 5(a) and 5(b) are Gaussian fits, respectively, to the atomic Hf 5d, 6s, and 6p features, and the band edge defects for the 1.5 nm thick HfO_2 film on Ge(100) annealed to 800 °C. The x-ray energies of the two defect features, and the lower e_g state in the Gaussian fit are essentially the same as those in derivative spectra, as are the energy differences. These comparisons validate the use of both approaches for characterizing average defect state energies, and their differences with respect to intrinsic bonding states of HfO_2.

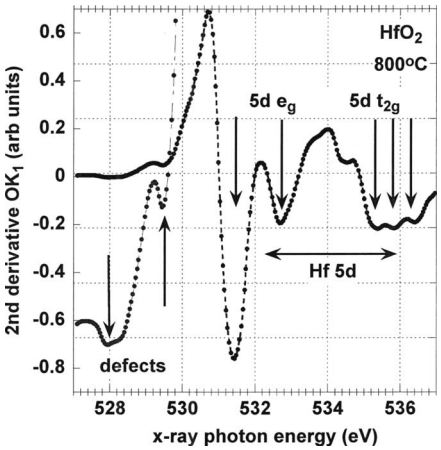

FIG. 4. Second derivative O K_1 edge spectrum for a 1.5 nm thick HfO_2 film on Ge(100) annealed to 800 °C, indicating Jahn-Teller split conduction band 5d states, and two band edge defects in a 10× scaled insert.

Figure 6 is a plot of the relative strengths of the defect features scaled to the combined strengths of the two Hf 5d e_g features as determined from the Gaussian fits for O K_1 spectra. This plot includes data for (i) deposition of HfO_2 on Ge(111), and, (iii) deposition of 2 nm HfO_2/1.5 nm HfSiON stacked film also on Ge(111); the dashed lines are included to indicate the trends in these data. There are several important

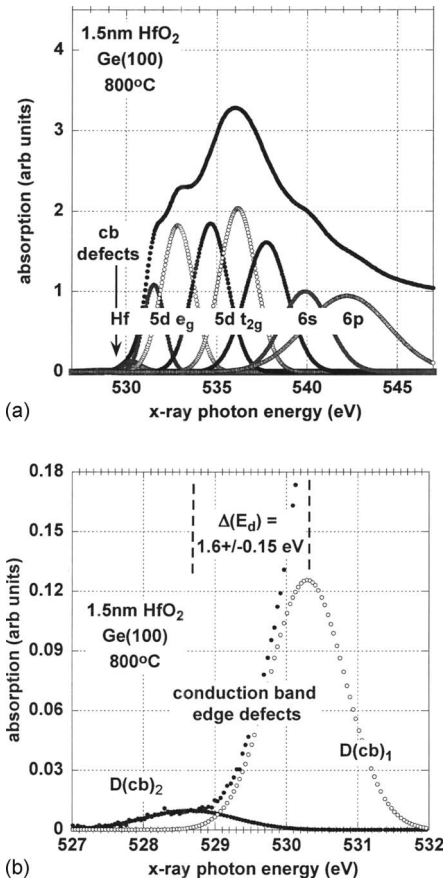

FIG. 5. O K_1 spectra for HfO_2 on Ge(100) annealed to 650 °C: (a) Gaussian fits to Hf 5d, 6s, and 6p features; and (b) Gaussian fit to band edge defects.

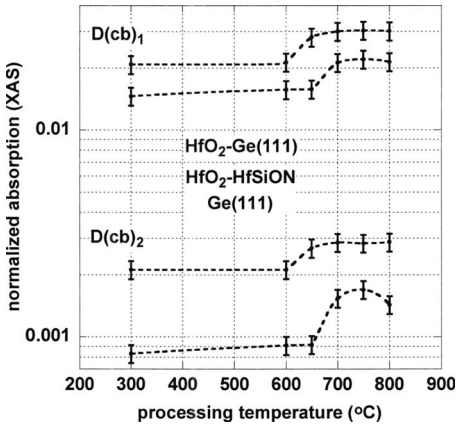

FIG. 6. Relative concentrations of defects for HfO_2 on Ge(111) and stacked HfO_2/HfSiON, also on Ge(111), as function of processing temperature. The dashed lines indicate trends in the data.

trends to note: (i) the qualitative changes in the defect densities for anneals >600 °C are the same for each of the two defect features as indicated by the respective trend lines for $HfO_2(100)/Ge(100)$ and $HfSiON/HfO_2/Ge(100)$ even though the relative increases occur a higher annealing temperature when HfSiON layers are included between the Ge substrate and the HfO_2 films.

Figure 7 indicates a fit to depth-resolved cathodoluminesce (DRCLS) data for a thick HfO_2 film on SiON/Si annealed to 900 °C.[23] The arrows indicate transitions between defect states that have been extracted from analysis of the XAS data presented above. These assignments are developed in the energy band diagrams in Fig. 8 which have been constructed from a combination of XAS, SXPS, and visible-vacuum ultraviolet spectroscopic ellipsomentry studies that have revealed pair defects, consistent with a divacancy defects, rather than monovacancy defects as suggested prior to the identification of paired valence and conduction band defects.[7,17]

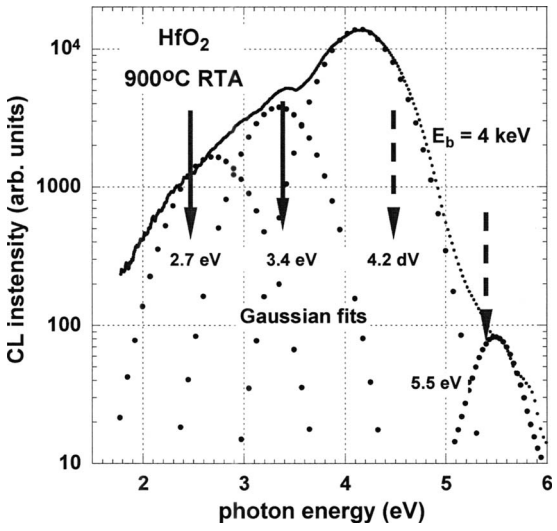

FIG. 7. Gaussian fits to four transition bands in the DRCLS for E_b=4 keV from a 100 nm thick HfO_2 film a 900 °C annealing.

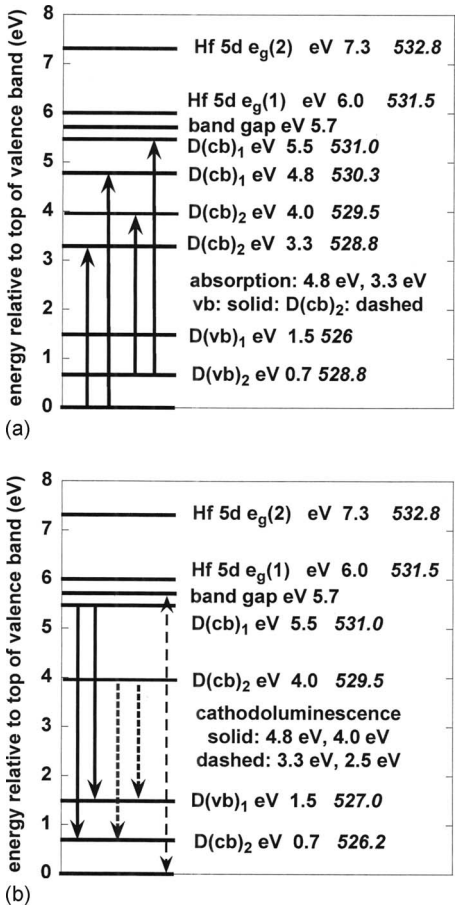

FIG. 8. Band edge defect feature energies derived from XAS data, including a conversion of the x-ray photon energies to energies equivalent to band gap transition energies based on linear scaling of the respective e_g d-state doublets: (a) transitions in black, including $D(cb)_1$ and $D(cd)_2$ energies, are referenced to valence band edge, whereas transitions in blue, are referenced to filled defect state energies; and (b) radiative defect level transitions in DRCLS in blue.

Figure 8 summarizes band edge defect features derived from spectroscopic data from XAS experiments, including a conversion of the x-ray energies to equivalent band gap transition energies based on linear scaling of the respective e_g d-state doublets. It is important to recognize that these are transition state energies for absorptions, and that they include hole final state effects; the localization of the hole on 1s core level states for the XAS spectra, and on valence band edge O $2p$ π nonbonding states in the vis VUV SE spectra. Scaling the impurity state energies in Fig. 8(a) is based an implicit assumption that they are associated with transitions from the top of the valence band. A better approximation, consistent with d-state localization is assume that the impurity absorptions must be attributed to intra-atomic transitions of the transition metal atom states that form the occupied and unoccupied states of the divacancies. This raises the conduction band edge defect state energies by ~0.7 eV. A test of these two assumptions is to compute the average crystal-field (C-F) splittings of the respective models. These are 2.95 and 3.65 eV, respectively. The C-F splitting from XAS is 3.6 ± 0.1 eV, favoring the intra-atom model. Based on this

energy level diagram, the defect absorptions are associated with transitions that originated in the lowest occupied valence band edge defect doublet state, $D(\mathrm{vb})_2$, and terminate in the two unoccupied states at the conduction band edge, $D(\mathrm{cb})_2=3.3$ eV, and $D(\mathrm{cb})_1=4.8$ eV. As demonstrated in Fig. 8(b), the intra-impurity level excitation model is consistent with cathodoluminescence studies done in collaboration with the Brillson group at The Ohio State University.[23]

VI. SUMMARY

This article has demonstrated a novel process sequence that shows promise for fabrication, initially of *n*MOSCAPs and *p*MOSCAPs with equally low intrinsic defect densities, both at the Ge-dielectric interfaces and within the bulk of the Hf-based dielectrics: (i) HfO_2, (ii)a high Si_3N_4 content Hf Si oxynitride dielectrics, $(HfO_2)_{0.3}(SiO_2)_{0.3}(Si_3N_4)_{0.4}$, (HfSiON); and (ii) dual layer or stacked HfO_2/HfSiON dielectrics. The HfO_2 films are direct contact with the Ge substrate, and the interfacial bonding is through a monolayer of Ge–O–Hf bonding; the HfSiON films are also in direct contact with the Ge substrate, with interfacial bonding arrangements, Ge–O–Si, and Ge–O–Hf. Finally, HfSiON layer of the dual layer dielectric HfO_2/HfSiON plays the role of an ITR, with interfacial bonding essentially the same as for single layer HfSiON.

The motivation for elimination completely native Ge ITRs, e.g., GeO_2, GeON, and Ge_3N_4, and the like, derives from measurements of the band gaps of GeO_2 and Ge_3N_4, and the integration of these band gaps into interfacial band alignment diagrams that indicate conduction band offset energies (CBOEs) which are smaller than those of the high-*K* dielectric HfO_2, and other Hf and Zr-based high-*K* dielectrics as well.

This article has relied on synchrotron based spectroscopies, mostly near edge XAS, and XPS to probe conduction states, and conduction and valence band edge defects, tracking changes in interface and film bonding as function of processing temperature. These measurements have identified a novel process sequence that defines a possible pathway to low defect densities, at Ge-dielectric interfaces and within the dielectric films addressed in this article. The most important aspects of this processing are (i) the implementation of a Ge wafer cleaning process that utilizes weakly acidic, and basic steps, (ii) passivation of the Ge surface by a remote plasma assisted nitridation process designed to prevent formation of Ge–O bonds during deposition of HfO_2 and HfSiON dielectrics, (iii) rapid thermal annealing in an Ar ambient at temperatures between 600 and 800 °C (in 50 °C degree increments), and tracking changes in conduction band final states, and conduction and valence band edge defects by XAS and XPS in order to (i) ensure complete elimination of the Ge–N created during the RPAN process; and (ii) to minimize reactions between the Ge substrates and the non-native Ge dielectrics in constant with the Ge substrate. These spectroscopic studies have identified a 50 °C difference in optimum processing for direct bonding HfO_2 to Ge, 575–625 °C, and the bonding of HfSiON to Ge, 625–675 °C, as stand alone dielectric, and an ITR for a HfSiON/HfO_2 stacked dielectric. Test devices are being fabricated using the optimized processing steps identified above, to determine, if the spectroscopic characterizations that apply to bulk defects apply to MOS gate stack structures, i.e., whether interface traps and/or fixed charge are more important than bulk defects this article has addressed used advanced spectroscopic techniques.

Finally, and a by-product of the spectroscopic studies, we have refined an energy level diagram of band edge states, and conduction and band edge defects. This diagram takes into recognizes the fact absorption processes give transition energies, which are not described by a one electron framework. This is done within the framework of symmetry adapted linear combinations of atomic states using the methods introduced by Cotton.[12]

ACKNOWLEDGMENTS

The authors acknowledge the excellent spectroscopic facilities for (i) the XAS measurements at the Stanford Synchrotron Research Laboratory and the assistance of Jan Lüning, Ben Wallace and Dennis Nordlund in these measurements, and (ii) the SXPS (XPS) measurements at the National Synchrotron Light Source at the Brookhaven National Laboratory. One of the authors (G.L.) acknowledges support from the Air Force Office of Scientific Research in MURI that is administered through Vanderbilt University, and from a grant from the Semiconductor Research Corporation.

[1]C. O. Chui *et al.*, J. Appl. Phys. **97**, 113518 (2005).
[2]C. O. Chui, F. Ito, and K. Saraswat, IEEE Trans. Electron Devices **53**, 1501 (2006).
[3]S. Takagi *et al.*, Microelectron. Eng. **84**, 2314 (2007).
[4]T. Krishnamohan *et al.*, Microelectron. Eng. **84**, 2063 (2007).
[5]R. S. Johnson, H. Niimi, and G. Lucovsky, J. Vac. Sci. Technol. A **18**, 1230 (2000).
[6]G. Lucovsky, G. S. Lee, and J. P. Long, Appl. Surf. Sci. **254**, 7933 (2008).
[7]G. Lucovsky, Microelectron. Eng. **84**, 2259 (2007).
[8]G. Lucovsky *et al.*, Jpn. J. Appl. Phys., Part 1 **46**, 1899 (2007).
[9]G. Lucovsky, J. Mol. Struct. **838**, 187 (2007).
[10]D. E. Aspnes and A. A. Studna, Appl. Phys. Lett. **39**, 316 (1981).
[11]T. Mori and D. E. Aspnes, Thin Solid Films **455**, 33 (2004).
[12]F. A. Cotton, *Chemical Applications of Group Theory*, 2nd ed. (Wiley Interscience, New York, 1963) Chap. 8.
[13]10 S. Wright, S. Feeney, and R. C. Barklie, Microelectron. Eng. **84**, 2378 (2007).
[14]L. Fleming *et al.*, J. Appl. Phys. **102**, 033707 (2007).
[15]R. Vasic *et al.* (unpublished).
[16]X-ray Data Booklet, Lawrence Berkeley National Laboratory, LBNL Pub-490 Rev 2, January 2001.
[17]G. Lucovsky *et al.*, in *SiGe, Ge and Related Compounds 3: Materials Processing and Devices*, edited by D. Harame *et al.* (The Electrochemical Society, Pennington, NJ, 2008), p. 381.
[18]K. B. Chung *et al.*, Appl. Phys. Lett. **93**, 182903 (2008).
[19]S. V. Hattangady *et al.*, Appl. Phys. Lett. **57**, 581 (1990).
[20]S. V. Hattangady *et al.*, J. Appl. Phys. **71**, 3842 (1992).
[21]K. Saraswat *et al.*, *SiGe, Ge and Related Compounds 3: Materials Processing and Devices*, edited by D. Harame *et al.* (The Electrochemical Society, Pennington, NJ, 2008), p. 3.
[22]*Handbook and Chemistry and Physics*, 33rd ed. (CRC, Cleveland, 1952), p. 498.
[23]Y. M. Strzhemechny *et al.*, J. Vac. Sci. Technol. B **26**, 232 (2008).